NEURAL REGENERATION RESEARCH
October 2015, Volume 10, Issue 10
www.nrronline.org

RESEARCH ARTICLE

The longitudinal epineural incision and complete nerve transection method for modeling sciatic nerve injury

Xing-long Cheng[1], Pei Wang[1], Bo Sun[1], Shi-bo Liu[1], Yun-feng Gao[1], Xin-ze He[2], Chang-yu Yu[1,*]

1 Department of Hand and Foot Surgery, Affiliated Hospital of Chengde Medical University, Chengde, Hebei Province, China
2 Graduate School of Chengde Medical University, Chengde, Hebei Province, China

***Correspondence to:**
Chang-yu Yu, M.D., cdgkwp@sina.com.

orcid:
0000-0003-4107-2265 (Chang-yu Yu)

doi: *10.4103/1673-5374.167767*
http:*//www.nrronline.org/*

Accepted: *2015-08-06*

Abstract

Injury severity, operative technique and nerve regeneration are important factors to consider when constructing a model of peripheral nerve injury. Here, we present a novel peripheral nerve injury model and compare it with the complete sciatic nerve transection method. In the experimental group, under a microscope, a 3-mm longitudinal incision was made in the epineurium of the sciatic nerve to reveal the nerve fibers, which were then transected. The small, longitudinal incision in the epineurium was then sutured closed, requiring no stump anastomosis. In the control group, the sciatic nerve was completely transected, and the epineurium was repaired by anastomosis. At 2 and 4 weeks after surgery, Wallerian degeneration was observed in both groups. In the experimental group, at 8 and 12 weeks after surgery, distinct medullary nerve fibers and axons were observed in the injured sciatic nerve. Regular, dense myelin sheaths were visible, as well as some scarring. By 12 weeks, the myelin sheaths were normal and intact, and a tight lamellar structure was observed. Functionally, limb movement and nerve conduction recovered in the injured region between 4 and 12 weeks. The present results demonstrate that longitudinal epineural incision with nerve transection can stably replicate a model of Sunderland grade IV peripheral nerve injury. Compared with the complete sciatic nerve transection model, our method reduced the difficulties of micromanipulation and surgery time, and resulted in good stump restoration, nerve regeneration, and functional recovery.

Key Words: *nerve regeneration; peripheral nerve; sciatic nerve injury; animal models; longitudinal epineural incision; Sunderland IV; nerve regeneration and repair; rats; neural regeneration*

Funding: *This study was supported by a grant from the Plan of the Department of Science and Technology of Hebei Province of China, No. 142777105D.*

Cheng XL, Wang P, Sun B, Liu SB, Gao YF, He XZ, Yu CY (2015) The longitudinal epineural incision and complete nerve transection method for modeling sciatic nerve injury. Neural Regen Res 10(10):1663-1668.

Introduction

Peripheral nerve injury can result in severe sensory and motor dysfunction, and remains an urgent medical challenge. The aim of the present study was to establish a suitable model of peripheral nerve injury for the study of nerve regeneration and repair. Methods of modeling nerve injury are improving continually; in addition to face validity, however, neuropathophysiology, neuroimmunology and pharmacology should also be considered when choosing a model in which to study nerve injury: Does the model replicate the mechanisms of injury and the extent of damage? Is the model fully operable and repeatable? Does it allow for control of the effects of systematic error on experimental intervention during model establishment?

Models of peripheral nerve injury can be established by exact or inexact methods. Complete sciatic nerve transection is a typical exact injury method. Its advantages are that the nerve fibers and epineurium are completely transected, without a microscope, and the injury severity is identical across nerve fibers. Santiago Ramón y Cajal first described the transection method in his Nobel Prize acceptance speech in 1906 (Savastano et al., 2014); however, limitations of the repair techniques and postoperative measurements he proposed in a model of Sunderland grade V injury meant satisfactory results were not obtained. With the rapid development of microscopy (Lundborg, 2000) and methodological improvements (Wall et al., 1974; Himes, 1989; Tandrup et al., 2000), it has become possible to conduct epineural repairs or nerve grafts under the microscope. However, poor fiber alignment, fibrosis and scar formation often result in poorly replicable results (Tos et al., 2011; Stdfano, 2015). Scarring is the biggest obstacle to replicating a model using this method. Autologous, allogeneic or artificial materials have been used to create sleeves or scaffolds to reduce the tension caused by epineural repair and improve stump anastomosis (James et al., 2010; Deal et al., 2012; Subramanian, 2012; Zhang et al.,

2013), but outcomes have not been ideal (Siemionow, 2010). Inexact injury methods mean that the extent and severity of the damage are variable or uncertain. Advantages of these methods are that they tend to be simple, and nerve regeneration and repair are often good. However, injury falls between Sunderland grades I and III, varying widely in severity and extent. Common models include nerve crush, for different degrees of damage to structure and function (Gutmann et al., 1943), severe nerve crush injury, in which the strength and duration of the crush are greater than in the mild crush model (Chell et al., 1992; Bridge et al., 1997), and freezing injury models (James, 1991). Additionally, to avoid mechanical damage, ischemia-reperfusion injury can be induced (Jia et al., 1999), which is limited to Sunderland grade II injury.

Here, we present a novel method for modeling peripheral nerve injury, characterized by precise damage severity and scope, and compare it with the complete sciatic transection model. We established the model in accordance with the anatomic features of the peripheral nerve. Transection of the nerve fibers *via* a small longitudinal incision in the epineurium induces Sunderland grade IV peripheral nerve injury, but limits the degree of epineural injury. The method avoids stump rotation and prevents the formation of a space induced by epineural retraction, as seen after complete transection, because retraction tension is parallel to the long axis. Our method solves the problem of reverse alignment and tension anastomosis of the nerve stump, simplifies the surgical technique, and improves repeatability of model induction. Furthermore, the independent environment of the epineurium is preserved, protecting the regenerating nerve fibers from extrinsic factors.

Materials and Methods

Animals

A total of 64 specific-pathogen-free male Sprague-Dawley rats, aged 12 weeks and weighing 250–275 g, were provided by Vital River Laboratories, Beijing, China (animal license No. SCXK (Jing) 2012-0001). They were housed in at 23 ± 2 °C, under a 12-hour light/dark cycle and with free access to food and water. All surgery was performed under anesthesia, and all efforts were made to minimize the pain and distress of the animals. The investigation conformed to the Guide for the Care and Use of Laboratory Animals published by the US National Institutes of Health (NIH publication No. 85-23, revised 1996), and the protocol was approved by the Animal Care Committee of Chengde Medical University, China. All rats were acclimated for 2 weeks before surgery.

Establishment of a rat model of sciatic nerve injury

Sixty-four rats were equally and randomly divided into an experimental group (longitudinal epineural incision and nerve transection method) and a control group (complete sciatic transection method). Rats were deprived of food and water for 8 hours prior to surgery. They were then anesthetized intraperitoneally with 4% chloral hydrate (10 mL/kg), and placed in the prone position. The right hindlimb was shaved and disinfected with an iodophor.

In the experimental group, a skin incision approximately 3-cm-long was made in the posterolateral right hindlimb, and the intermuscular septum was bluntly dissected. Using a light microscope at 15× magnification (LEL-6A; Zhongtian Optical Instrument Co., Ltd., Zhenjiang, China), the sciatic nerve was exposed and dissociated, and a 3-mm longitudinal incision was made in the epineurium, 1 cm inferior to the piriformis, using microscissors (Cheng-He Microsurgical Instruments Factory, Ningbo, China). The exposed nerve fibers were isolated using noninvasive microforceps (Cheng-He Microsurgical Instruments Factory), and sharply transected under direct vision. The two nerve stumps were placed back together if the epineurium remained intact. No retraction or

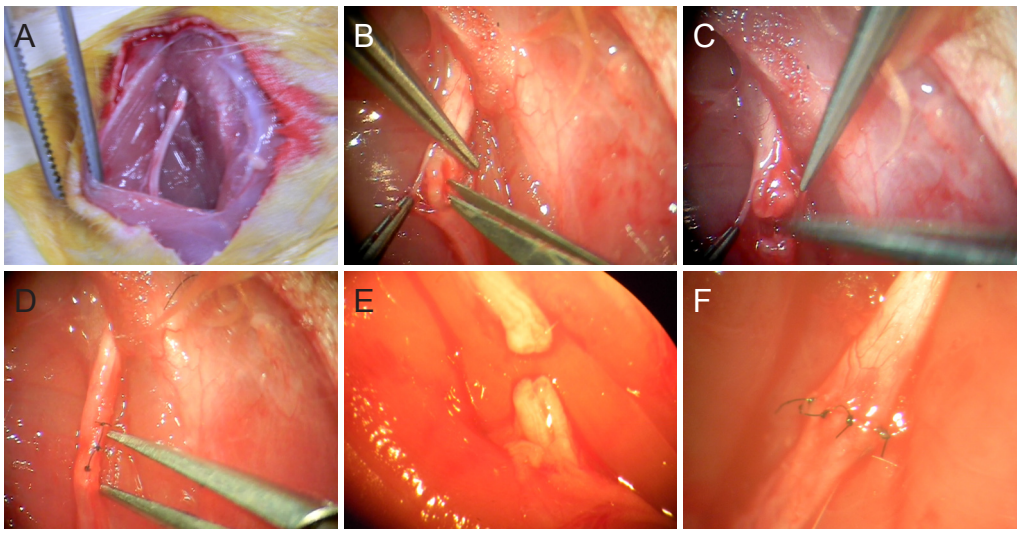

Figure 1 Construction of a rat model of sciatic nerve injury
(A) A longitudinal incision on the posterolateral right hindlimb and exposure of 3-cm sciatic nerve, from pelvic cavity to bifurcation of tibial and common peroneal nerves. (B–D) Experimental group: a 3-mm longitudinal incision was made in the epineurium, then the nerve fiber was completely transected, without a microscope, to make sure the epineurium was intact. The epineurium was closed with three 9-0 noninvasive stitches. (E, F) Control group: sciatic nerve was completely transected, then the epineurium was closed with six 9-0 noninvasive stitches. B–F, 15× magnification.

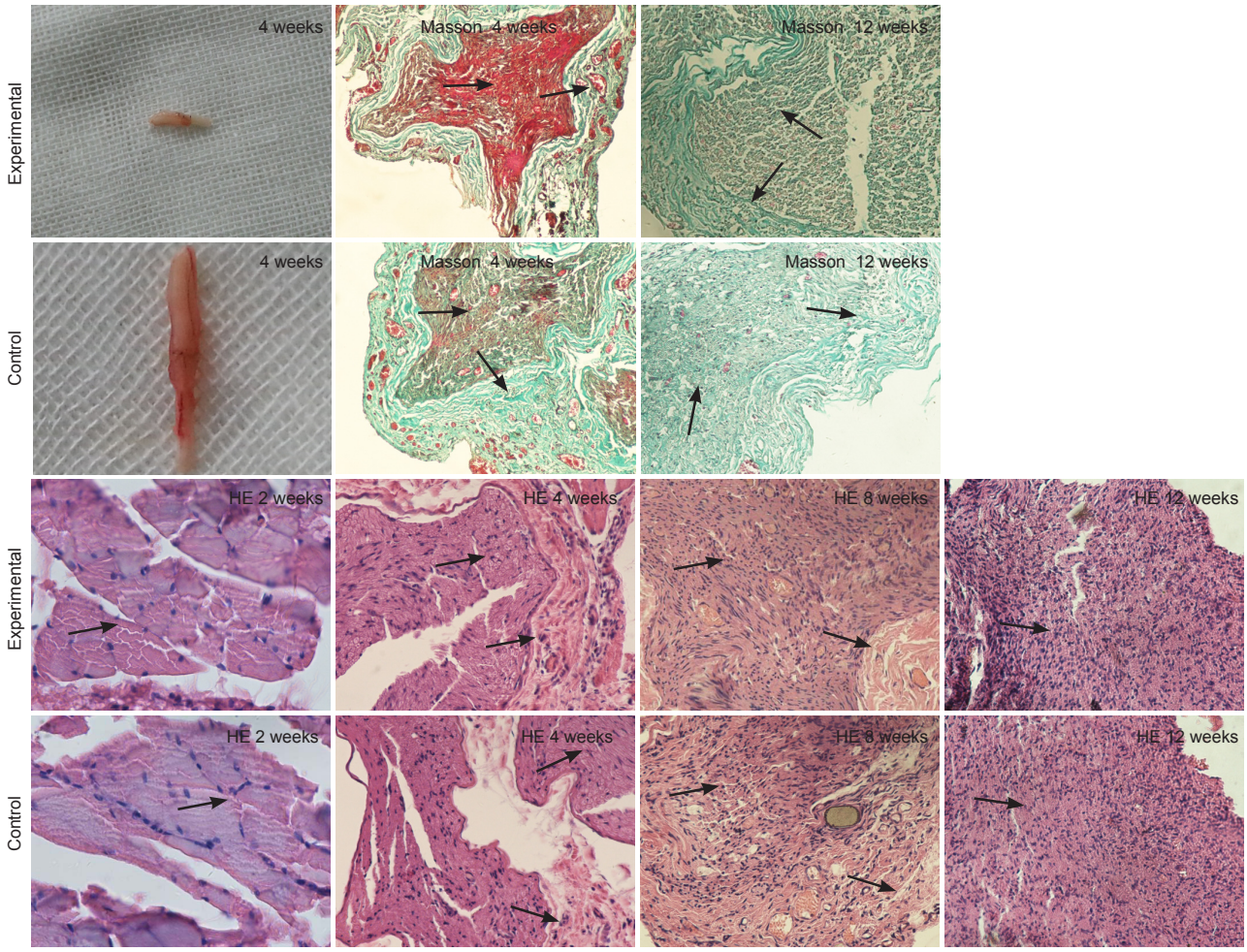

Figure 2 Histological changes in injured sciatic nerve.
In the control group, 4 weeks after surgery, scar adhesions were found at the anastomotic site, and the diameter of the distal nerve appeared thin. Gross observation of the experimental group showed that there was no obvious adhesion of scar to connective tissue at the anastomotic site, and proximal and distal nerve diameters were identical. Masson's trichrome staining (× 200) at 4 weeks revealed collagen fibers (arrows) and angiogenesis, proliferation of the collagen fibers in the perineurium and endoneurium, and lightly-stained axons. In the experimental group, the number of collagen fibers (arrows) and blood vessels was greater than in controls, and the regenerated axons were stained red. At 12 weeks, in the control group, the epineurium was disordered with an unclear boundary; collagen fiber hyperplasia was seen in the perineurium and endoneurium (arrows); and Schwann cell nuclei were arranged in a disorderly manner. In contrast, in the experimental group, no collagen fiber hyperplasia was found in the epineurium, perineurium or endoneurium (arrows), and Schwann cell nuclei appeared more dense and regular. Hematoxylin-eosin (HE) staining revealed that at 2 weeks in both groups, axons broke or disappeared, and the myelin sheaths disintegrated (× 400). At 4 weeks, a large number of inflammatory cells (arrows) had infiltrated. Axons and myelin sheaths disappeared. Vacuoles were seen in nerve fibers, and the outer membrane became thickened. Old and new inflammatory cell infiltration and remyelination were visible (× 100). At 8 weeks, in the control group, many axons had started to regenerate (arrows), but with a disorderly arrangement, and the epineurium showed a small amount of inflammatory cell infiltration. Conversely, in the experimental group, axons had started to regenerate (arrows) and were uniformly distributed, and no inflammatory cell infiltration in the epineurium was seen in the experimental group (× 100). At 12 weeks, axons showed notable regeneration (arrows) in both groups. There were more regenerated axons, and the axons were more uniform in the experimental group than in the control group (× 100).

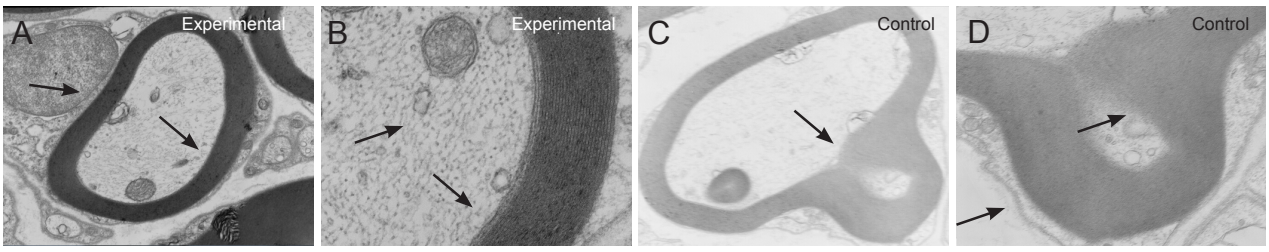

Figure 3 Ultrastructure of injured sciatic nerve in rats at 12 weeks after surgery (transmission electron microscope).
(A, C) At 500× and 7,500× magnification, myelin sheaths (arrows) were normal and dense in the experimental group, but the regenerated myelin sheaths (arrows) were abnormal and sparse in the control group. (B, D) At 15,000× magnification, dense myelin sheaths and many distinct regenerated axons, microfilaments and microtubules (arrows) were visible in the experimental group. In comparison, in the control group, the regenerated myelin sheaths were sparse and abnormal, axons were very small, there were fewer microfilaments and microtubules than in the experimental group, and edema was apparent.

Table 1 Sciatic functional index in rats with sciatic nerve injury

	Weeks after surgery				
Group	0	2	4	8	12
Experimental	–12.02±3.13	–85.72±3.25	–68.26±2.33	–41.62±3.12*	–25.46±2.23*
Control	–11.84±3.32	–86.24±4.32	–79.27±137	–60.33±2.26	–45.27±2.68

Sciatic functional index: 0, normal; −100, complete impairment. *$P < 0.01$, *vs.* control group (mean ± SD, $n = 8$, one-way analysis of variance and Student-Newman-Keuls test).

Table 2 Motor nerve conduction velocity (m/s) of injured sciatic nerve

	Weeks after surgery			
Group	0	4	8	12
Experimental	65.12±1.34	32.96±2.33*	38.77±1.02*	46.34±1.52*
Control	64.81±1.12	19.22±1.35	22.29±1.36	26.32±1.48

Motor nerve conduction velocity = distance between two stimulating electrodes / action potential latency (conduction velocity, m/s). *$P < 0.01$, *vs.* control group (mean ± SD, $n = 8$, one-way analysis of variance and Student-Newman-Keuls test).

torsion was observed and the stump fitted well without any space. The longitudinal epineural incision was closed with three 9-0 noninvasive sutures (**Figure 1**).

Surgery in the control group was identical to the experimental group, except that the nerve was transected completely without first opening the epineurium. The stumps were trimmed and the epineurium was closed under a microscope, using six 9-0 noninvasive sutures (**Figure 1**).

Behavioral analysis

Eight rats were chosen at random from each group the day before surgery and 0, 2, 4, 8 and 12 weeks after surgery. Sciatic functional index (SFI) was assessed as described previously (de Medinaceli, 1982), and calculated according to the following formula: −38.3 [(EPL−NPL)/NPL] + 109.5 [(ETS−NTS)/NTS] + 3.3 [(EIT−NIT)/NIT]−8.8, where PL refers to print length (the distance between heel and toe), TS refers to toe spread (the distance between the first and fifth toes), IT refers to intermediary toe spread (the distance between the second and fourth toe), E refers to the experimental foot, and N refers to the normal (contralateral) foot. SFI = 0 indicates normal behavior and −100 indicates complete impairment.

Electrophysiological analysis

Eight rats from each group were obtained at 4, 8 and 12 weeks after surgery. Motor nerve conduction velocity was measured using a Medtronic Keypoint electromyography machine (Keypoint Workstation 31A06; Alpine BioMed ApS, Skovlunde, Denmark). All rats were anesthetized with 4% chloral hydrate, placed in the prone position, and the skin over the site of the injury was disinfected. An incision was made to expose the injured sciatic nerve. A recording electrode was inserted into the soleus muscle, and a grounding electrode was placed on the tail. Two stimulating electrodes were placed at the proximal ischial tuberosity and distal sciatic nerve branch, 2 cm apart. A superstrong stimulus (10 mA) was applied, and the motor nerve conduction velocity was calculated as the distance between the two stimulating electrodes/action potential latency (conduction velocity, m/s).

Hematoxylin-eosin staining

At 2, 4, 8 and 12 weeks after surgery, eight rats from each group were sacrificed with an overdose of 4% chloral hydrate anesthesia. Approximately 5 mm of the sciatic nerve at the distal anastomotic site was fixed in 10% neutral formalin for 24 hours, dehydrated through a graded alcohol series, embedded in paraffin, and cut into 6-μm transverse sections. The sections were dewaxed with xylene, hydrated through a graded alcohol series, stained with hematoxylin, treated with acidic alcohol, immersed in running water, stained with eosin, dehydrated, permeabilized and mounted. The tissue was viewed under a light microscope (BH-2; Olympus, Tokyo, Japan) to examine myelin degeneration and regeneration.

Masson's trichrome staining

At 4 and 12 weeks post surgery, four rats from each group were sacrificed by anesthesia with 4% chloral hydrate. Sciatic nerve sections were prepared as described above, and Masson's trichrome staining was performed using a kit (KeyGEN Biotechnology Co., Ltd., Nanjing, China), according to the manufacturer's instructions. Axon regeneration and scar formation were observed under a light microscope (BH-2; Olympus).

Transmission electron microscopy

At 12 weeks post surgery, four rats were randomly obtained from each group and sacrificed by anesthesia with 4% chloral hydrate. A 5-mm length of the right sciatic nerve at the distal anastomotic site was fixed in 4% glutaral at 4°C for 24 hours, then in 1% osmic acid, embedded in epoxy resin, and cut into ultrathin sections for uranyl acetate and lead citrate staining. Axon regeneration and myelination were observed under a transmission electron microscope (H-7500; Hitachi, Tokyo, Japan).

Statistical analysis

Measurement data are expressed as the mean ± SD, and were analyzed using SPSS 17.0 software (SPSS, Chicago, IL, USA). Groups were compared using one-way analysis of variance followed by the Student-Newman-Keuls test. $P < 0.05$ was considered statistically significant.

Results

General condition of rats with sciatic nerve injury

Right hindlimb paralysis was visible in both groups after surgery. At 1 week, the incisions were healed by first intention in both groups. At 2 weeks, toe swelling and ulceration were observed on the affected side, so the wound surfaces were washed with physiological saline and coated with saturated aqueous picric acid to prevent self-mutilation. The right lower limb ulcers had healed in the experimental group after 6 weeks and in the control group after 8 weeks. In the experimental group, the earliest recovery time of autonomous motion was 4 weeks, with a mean of 5 weeks. In the control group, the earliest recovery time of autonomous motion was 6 weeks, with a mean of 8 weeks.

Histological changes in injured sciatic nerve

At 2 and 4 weeks after surgery, no significant differences were observed in the histology of the injured sciatic nerve between the experimental and control groups. There was distinct Wallerian degeneration, considerable inflammatory cell infiltration, and myelin sheath disintegration. Vacuoles were present in nerve fibers and the outer membrane was thickened. At 8 and 12 weeks, Schwann cell proliferation, myelinated nerve fiber growth and neuritogenesis were noticeable, but myelination and capillary formation were incomplete in the experimental group (**Figure 2**). After Masson's trichrome staining, collagen fibers appeared green, axons red, and nuclei dark blue. Light microscopy did not reveal any significant differences in epineural collagen fibers at 4 weeks after surgery between the two groups. However, at 12 weeks, fewer collagen fibers were observed in the experimental group than in the control group. Furthermore, axon regeneration was better in the experimental group than in the control group (**Figure 2**).

Behavioral changes in rats with sciatic nerve injury

Sciatic nerve function was normal in the two groups before surgery. From 0–3 weeks after surgery, the right lower limbs presented varying degrees of dysfunction in both groups, with no statistically significant difference between the two groups. At 4–8 weeks, motor function of the right lower limb was restored in both groups, but SFI was better in the experimental group than in the control group ($P < 0.01$; **Table 1**).

Electrophysiological changes in the injured sciatic nerve

Electrophysiology was normal in both groups during the surgery, with no statistical difference between the groups. However, at 4, 8 and 12 weeks after surgery, neuronal conduction was faster in the experimental group than in the control group ($P < 0.01$; **Table 2**).

Ultrastructure of injured sciatic nerve

At 12 weeks after surgery, transmission electron microscopy revealed that animals in the experimental group had more myelinated nerve fibers than those in the control group. The regenerated myelin sheaths were normal and intact, with a tight lamellar structure. The axon membrane was closely adjacent to the myelin membrane. In the control group, the regenerated myelin sheaths were sparse, and edema was apparent; axons were very small, with few microtubules and microfilaments (**Figure 3**).

Discussion

Stability, operability and repeatability are the basic requirements for models of peripheral nerve injury. The classic method of complete sciatic transection, although accurate (Savastano et al., 2014), requires a high level of surgical skill, which affects its operability. We therefore proposed a new method of model establishment: the longitudinal epineural incision and nerve transection method. The method overcomes the limitations of the complete transection model, and accurately replicates nerve injury *via* a small epineural incision combined with complete transection of axons, endoneurium and perineurium, equivalent to a Sunderland grade IV injury (Chhabra, 2014). Our results demonstrate that at 2 and 4 weeks after surgery, Wallerian degeneration, inflammatory cell infiltration, myelin disintegration, nerve fibers with vacuoles, thickened epineurium and myelin degeneration occurred in both groups after injury, in addition to sensory and motor dysfunction. At 2 weeks, ulcers appeared in denervated areas and remained until at least 4 weeks. The longitudinal epineural incision and nerve transection method differs from incomplete injuries, avoiding the variability in Sunderland grades II–III obtained with such methods (Moradzadeh et al., 2010; Bozkurt et al., 2011), as well as the complexity and instability that occur after inaccurate injuries such as milling machine injury and ischemia-reperfusion injury (Jia et al., 1999; Savastano et al., 2014).

The longitudinal epineural incision and nerve transection method minimizes damage to the epineurium and improves operational skills during model induction. The theory of production is derived from the anatomical characteristics of the peripheral nerve. There are tight, fibrous connections between the epineurium and perineurium, which provide the blood supply between fiber bundles, maintaining the stability of the structure, and preventing fiber bundle retraction and torsion. In the new model, these fibrous joints were transected and reset without the need for a microscope. No stump torsion or space induced by epineural retraction was found after the transection, because retraction tension was parallel to the long axis. This model requires only a small, longitudinal incision to be sutured for nerve repair. It is not necessary to locate epineural anastomosis according to the direction of blood vessels on the perineurium (Bozkurt et al., 2011). Our results confirmed that at 4–12 weeks after surgery, using the new method, myelinated nerve fibers had notably regenerated, scar formation was unremarkable, and the myelin sheaths were dense and regular. Furthermore, conduction velocity and the action potential conduction quality were noticeably better in the experimental group than in the control group. Together, these results indicate that the method presented here results in good peripheral nerve function and regeneration.

The self-contained space of the epineurium may reduce exogenous inflammatory cell invasion and scar formation induced by fibroblast activation, maintain nerve fiber regeneration, and avoid obstruction of nerve regeneration and neuroma formation (Smit et al., 2004). Masson's trichrome staining revealed a lack of collagen fiber hyperplasia in the epineurium at 12 weeks in the experimental group, and Schwann cell nuclei were dense and regular.

In summary, we have successfully established a nerve injury model using a longitudinal epineural incision with complete nerve transection. This method substantially reduces the difficulty and time required for the microoperation, obtains good stump anastomosis and nerve repair, elevates operability and stability of model establishment and use, and replicates a Sunderland grade IV injury. However, the longitudinal epineural incision and complete nerve transection method has some limitations, including the necessity for basic training in the micro-operation when the model is first used. The application of this model requires further characterization in the study of peripheral nerve injury.

Acknowledgments: *We are very grateful to Xiao-guang Wu, Li-qun Ren and Long Chen from the Institute of Basic Research, Chengde Medical College, China for their supports on basic experiment, and teachers from the Functional Experiment Center of Chengde Medical College, Room of Electromyogram of Affiliated Hospital of Chengde Medical University and Central Laboratory of Electron Microscopy of Hebei Medical University, China for their supports.*

Author contributions: *CYY and XLC participated in study concept and design. BS, SBL, YFG and XZH provided technical and material support. CYY, XLC and PW collected and analyzed data, ensured the integrity of the data, and wrote the paper. CYY and PW served as principle investigators, were in charge of paper authorization, and obtained the funding. All authors approved the final version of the paper.*

Conflicts of interest: *None declared.*

References

Bozkurt A, Dunda SE, O'Dey DM, Brook GA, Suschek CV, Pallua N (2011) Epineurial sheath tube (EST) technique: an experimental peripheral nerve repair model. Neurol Res 33:1010-1015.

Bridge PM, Ball DJ, Mackinnon SE (1997) Nerve crush injuries-a model for axonotmesis. Exp Neurol 127:284-290.

Chell LE, Seaher AV, Glisson RR, Davies H, Murrell GA, Anthony DC, Urbaniak JR (1992) The functional recovery of peripheral nerves following defined acute crush injuries. Orthop Res 10:657-664.

Chhabra A, Ahlawat S, Belzberg A, Andreseik G (2014) Peripheral nerve injury grading simplified on MR neurography: as referenced to Seddon and Sunderland classifications. Indian J Radiol Imaging 24:217-224.

Deal DN, Griffin JW, Hogan MV (2012) Nerve conduits for nerve repair or reconstruction. J Am Acad Orthop Surg 20:63-68.

de Medinaceli L, William J (1982) An index of the functional condition of rat sciatic nerve based on measurements made from walking tracks. Exp Neurol 77:634-637.

Geuna S (2015) The sciatic nerve injury model in pre-clinical research. J Neurosci Methods 243:39-46.

Gutmann E, Sanders FK (1943) Recovery of fibre numbers and diameters in the regeneration of peripheral nerves. J Physiol 101:489-518.

Himes BT, Tessler A (1989) Death of some dorsal root ganglion neurons and plasticity of others following sciatic nerve section in adult and neonatal rats. Comp Neurol 284:215-230.

James R, Toti US, Laurencin CT, Kumbar SG (2011) Electrospun nanofibrous scaffolds for engineering soft connective tissues. Methods Mol Biol 726:243-258.

Jia JP, Pollock M (1999) Cold nerve injury is enhanced by intermittent cooling. Muscle Nerve 22:1644-1652.

Kerns JM, Braverman B, Mathew A, Lucchinetti C, Ivankovich AD (1991) A comparison of cryoprobe and crush lesions in the rat sciatic nerve. Pain 47:31-39.

Lundborg G (2000) A 25-year perspective of peripheral nerve surgery:evolving neuroscientific concepts and clinical significance. Hand Surg Am 25:391-414.

Moradzadeh A, Brenner MJ, Whitlock EL, Tong AY, Luciano JP, Hunter DA, Myckatyn TM, Mackinnon SE (2010) A rodent model of sunderland third-degree nerve injury. Arch Facial Plast Surg 12:40-47.

Savastano LE, Laurito SR, Fitt MR, Rasmussen JA, Gonzalez Polo V, Patterson SI (2014) Sciatic nerve injury: a simple and subtle model for investigating many aspects of nervous system damage and recovery. J Neurosci Methods 227:166-180.

Siemionow M, Bozkurt M, Zor F (2010) Regeneration and repair of peripheral nerves with different biomatefials: review. Microsurgery 30:574-588.

Smit X, van Neck JW, Afoke A, Hovius SE (2004) Reduction of neural adhesions by biodegradable autocrosslinked hyaluronic acid gel after injury of peripheral nerves: an experimental study. J Neurosurg 101:648-652.

Subramanian A (2012) Axially aligned electrically conducting biodegradable nanofibers for neural regeneration. J Mater Sci Mater Med 23:1797-1809.

Tandrup T, Woolf CJ, Coggeshall RE (2000) Delayed loss of small dorsal root ganglion cells after transection of the rat sciatic nerve. Comp Neurol 422:172-180.

Tos P, Geuna S, Papalia I, Conforti LG, Artiaco S, Battiston B (2011) Experimental and clinical employment of end-to-side coaptation: our experience. Acta Nenrochir Suppl 108:241-245.

Wall PD, Gutnick M (1974) Properties of afferent nerve impulses originating from a neuroma. Nature 248:740-743.

Zhang Z, Kou Y, Yin X, Wang Y, Zhang P, Jiang B (2013) The effect of a small gap sleeve suture at the distal anastomosis of a nerve graft on promoting nerve regeneration and functional recovery. Artif Cells Nanomed Biotechnol 41:282-288.

Copyedited by Slone-Murphy J, Haase R, Wang J, Qiu Y, Li CH, Song LP, Zhao M